Quantum dynamics in driven sawtooth lattice under uniform magnetic field

Xiaoming Cai,[1,2] Shu Chen,[1] and Yupeng Wang[1]

[1]*Beijing National Laboratory for Condensed Matter Physics, Institute of Physics, Chinese Academy of Sciences, Beijing 100190, China*

[2]*State Key Laboratory of Magnetic Resonance and Atomic and Molecular Physics, Wuhan Institute of Physics and Mathematics, Chinese Academy of Sciences, Wuhan 430071, China*

(Received 7 June 2012; published 9 January 2013)

We study the Bloch-Zener oscillation, which is a superposition of Bloch oscillation and Landau-Zener tunneling between Bloch bands, for a quantum particle in a frustrated sawtooth lattice with and without uniform magnetic field. Under the single-band tight-binding approximation, the sawtooth lattice is a two-miniband system and may have a flat band structure. The presence of magnetic field can make the gap between two minibands close, and around the touch point the dispersion is an asymmetric Dirac cone. We analyze in detail the Landau-Zener tunneling and Bragg scattering in the Bloch-Zener oscillation and the effect of magnetic field. Our results also give a clear picture of the dynamical localization in real space induced by the flat band structure of the lattice.

DOI: 10.1103/PhysRevA.87.013607 PACS number(s): 03.75.Lm

I. INTRODUCTION

Bloch oscillation and Landau-Zener tunneling are fundamental transport phenomena of an object in periodic potentials [1–4]. Accelerated by a weak external constant force, an object undergoes a coherent periodic motion (Bloch oscillation) in the periodic potential, which is related to the formation of the energy spectrum of the Wannier-Stark ladder [5] and localized single-particle states. Tunneling to higher-order bands (Landau-Zener tunneling [2,3,6,7]) is responsible for Bloch oscillation damping and broadening of Wannier-Stark resonances for a stronger driving force. Bloch oscillation and Landau-Zener tunneling have been demonstrated in a number of experiments, for example, electrons in semiconductor superlattices [8], light pluses in photonic crystals [9,10], and cold atoms in an optical lattice [4]. For a multiband system, such as the system with the usual cosine-shaped potential, whose band gaps usually decrease rapidly as the energy increases, a cascade of Landau-Zener tunneling to higher-order bands would lead to the damping of the Bloch oscillation [11–13]. In order to study the steady interplay between Bloch oscillation and Landau-Zener tunneling, which is known as Bloch-Zener oscillation [14–16], a two-miniband system is needed. For such a system, the two minibands should be well separated from the upper ones, and the gap between these two minibands is small for large Landau-Zener tunneling probability. Because of the two Wannier-Stark ladder energy spectra with an offset between them, the Bloch-Zener oscillation is characterized by two time scales, i.e., the Bloch period and the period of Zener oscillation [14]. If the two periods are commensurate, the system will reconstruct at integer multiples of the Bloch-Zener time.

As one of the simplest frustrated models, the quantum Heisenberg antiferromagnet model on the sawtooth lattice has been extensively studied in recent decades [17–25] and has also an experimental realization in chemistry [26]. Under high magnetic fields, the spin sawtooth system has been found to exhibit various peculiar properties, for example, the macroscopic magnetization jump [27], residual entropy [28,29], and the enhanced magnetocaloric effect [24,30]. Due to recent progress in optical lattices for cold atoms [31–33] and in nanotechnology, which allows the fabrication of quantum-dot superlattices and quantum-wire systems with any type of lattice [34–36], flat-band ferromagnetism of Hubbard electrons in a sawtooth lattice also attracted much attention [37–39]. These systems also exhibit some peculiar properties, such as highly degenerate ground states constructed exactly by localized electrons and residual entropy, which are closely related to their flat band structures.

As the unit cell of the sawtooth chain contains two asymmetrical sites, its single-particle spectra consist of two branches, with one of the branches becoming a completely flat band [40] at a fine-tuning point of the hopping parameters along the baseline and zigzag path [see Fig. 1(a)]. A peculiar property related to the flat band is that the corresponding states in the flat band are localized. If the flat band is the lower band and partially filled, the ground states are highly degenerate with nonzero residual entropy. As most previous studies on the sawtooth lattice focused on the ground-state properties and thermodynamics for systems without magnetic field, the quantum dynamics in the sawtooth lattice is rarely studied. In this paper we shall study the dynamics of a quantum particle in the driven sawtooth lattice under a uniform magnetic field and explore the effect of the flat band on the single-particle dynamics. In the presence of a uniform magnetic field, the band structure of the sawtooth lattice is dramatically changed; for example, asymmetric Dirac cone in dispersion may appear for a particular magnetic field, and the gap between two bands is tunable by the change of the strength of the magnetic field. As a two-miniband system with possible partially flat Bloch bands and a tunable gap for Landau-Zener tunneling, one can expect that the dynamics of a particle in the driven sawtooth lattice will be affected by the specific band structure, for example, Landau-Zener tunneling and Bragg scattering happening at different times, and dynamical localization of a particle.

This paper is organized as follows. In Sec. II, we introduce the model and study the spectrum properties for the case without driving force. We present the Bloch bands under different parameter regions and discuss the influence of the magnetic field on the band structure. In Sec. III, we study the quantum dynamics of a single particle in the sawtooth under a driving force. The Landau-Zener tunneling and Bragg scattering in the Bloch-Zener oscillation are analyzed. A summary is given in the last section.

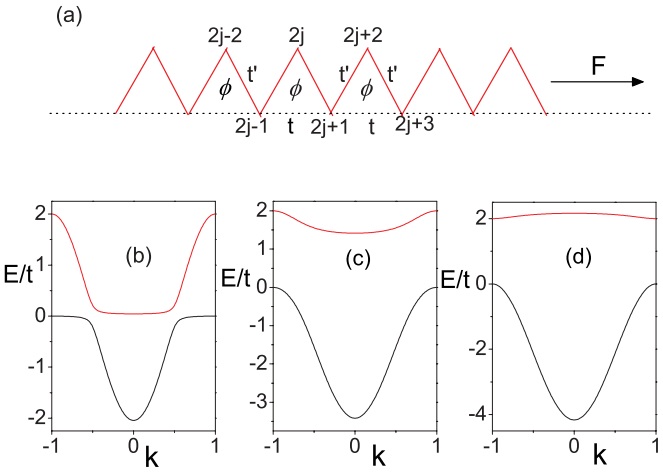

FIG. 1. (Color online) (a) The schema of the sawtooth lattice, driving force F, and magnetic flux ϕ. t is the hopping amplitude along the baseline (black dotted line), while t' is the hopping amplitude along the zigzag path (red solid line). The single-particle dispersion for the sawtooth lattice in the absence of driving force and magnetic flux with (b) $t'/t = 0.15$, (c) $t'/t = 1.1$, and (d) $t'/t = 1.5$. k is in units of $\pi/2$.

II. BLOCH BANDS FOR A SYSTEM WITHOUT DRIVING FORCE

Under Landau gauge $A_x = -By, A_y = 0$, the Hamiltonian of a driven sawtooth lattice reads

$$H = -t' \sum_j (e^{-i\phi\pi} c_j^\dagger c_{j+1} + \text{H.c.}) - t \sum_j (c_{2j-1}^\dagger c_{2j+1} + \text{H.c.}) - F \sum_j j n_j. \quad (1)$$

Here we neglect the off-diagonal terms of position operator $\hat{x}$ in the Wannier basis, $c_j^\dagger$ (c_j) is the creation (annihilation) operator of a quantum particle at site j, n_j is the particle number operator, and $t > 0$ ($t' > 0$) is the hopping amplitude along the baseline (zigzag path). For the rest of paper we set $t = 1$ to be the unit of energy. The parameter F is the strength of the driving force. The lattice spacing along the baseline is set to 2, and ϕ is the magnetic flux in each triangle, which is related to the magnetic field by $\phi = BS/\phi_0$. Here S is the area of a triangle, B is the strength of the magnetic field, and ϕ_0 is the magnetic flux quantum.

In this section, we study the spectral properties of the system without driving force ($F = 0$). The Hamiltonian with $F = 0$ can be formulated as a 2×2 matrix in terms of "spinor" $\vec{c}_k = [c_{A,k}, c_{B,k}]^T$ representing two different types of sites in the unit cell,

$$H = -\sum_k \vec{c}_k^\dagger \begin{bmatrix} 0 & t'(e^{i\pi\phi} + e^{i2k-i\pi\phi}) \\ t'(e^{-i\pi\phi} + e^{i\pi\phi-i2k}) & 2t\cos(2k) \end{bmatrix} \vec{c}_k, \quad (2)$$

where the sum runs over the first Brillouin zone $(-\pi/2, \pi/2]$, B represents the lattice sites in baseline, and A represents the others. The dispersion is given by

$$E_\pm = -t\cos(2k) \pm \sqrt{t^2\cos^2(2k) + 2t'^2[1 + \cos(2k - 2\phi\pi)]}. \quad (3)$$

The corresponding Bloch wave functions for both bands are given by

$$|\chi_\pm\rangle = \frac{1}{\sqrt{M_\pm}}(u c_{A,k}^\dagger + E_\pm c_{B,k}^\dagger)|0\rangle, \quad (4)$$

with $u = t'(e^{i\pi\phi} + e^{i2k-i\pi\phi})$ and $M_\pm = |u|^2 + E_\pm^2$.

First, we discuss in detail the properties of the dispersion for the system without magnetic field. When $\phi = 0$, the dispersion (3) reduces to the well-known dispersion of the sawtooth lattice [37–40]. We note that almost all previous works focus on the system with the special ratio $t'/t = \sqrt{2}$, for which the dispersion becomes

$$\varepsilon_+ = 2t, \quad \varepsilon_- = -2t[1 + \cos(2k)]. \quad (5)$$

Obviously, one of the Bloch bands is completely flat, and under the flat dispersion localized eigenstates can be formed, which are given by [40]

$$|\Gamma_j\rangle = \tfrac{1}{2}(c_{2j-1}^\dagger + c_{2j+1}^\dagger - \sqrt{2}c_{2j}^\dagger)|0\rangle. \quad (6)$$

For the general ratio t'/t, we classify the dispersion into three different types. (1) For the system with $0 < t'/t < 1$ [Fig. 1(b)], both bands are the V type. Landau-Zener tunneling does not happen at the edge of Brillouin zone and is separated from Bragg scattering against the usual case where both take place at the edge of the Brillouin zone ([14,41]). The gap for Landau-Zener tunneling, which happens between two bands at the same momenta, is defined as $\Delta = \min[E_+(k) - E_-(k)]$. For $0 < t'/t < 1$, $\Delta = 2t'\sqrt{2 - (t'/t)^2}$, with the corresponding momenta satisfying $\cos(2k) = -t'/t$. Notice that, when $t'/t \ll 1$, both bands are partially flat and Landau-Zener tunneling happens at $k \simeq \pm\pi/4$. (2) For the system with $1 \leqslant t'/t \leqslant \sqrt{2}$ [Fig. 1(c)], both bands are still the V type. But since $\cos(2k) = -t'/t$ has no solution, Δ gets its value at the edge of the Brillouin zone with $\Delta = 2t$. (3) For the system with $t'/t > \sqrt{2}$ [Fig. 1(d)], as the ratio becomes bigger than $\sqrt{2}$, the upper Bloch band changes into the Λ type, and $\sqrt{2}$ is a critical ratio which causes the flat Bloch band. Δ still gets its value at the edges of the Brillouin zone with $\Delta = 2t$. Landau-Zener tunneling and Bragg scattering happen at the same time.

In the presence of magnetic field, the time-reversal symmetry of the system is broken, and Bloch bands usually become asymmetrical. The dispersion for $1 - \phi$ is the mirror image of the case ϕ because $E(-k,\phi) = E(k, 1-\phi)$. We only study the spectral properties of the system with magnetic flux $\phi \in [0, 1/2]$. In Figs. 2(a)–2(c), we show dispersions for three different magnetic fluxes with $t'/t \ll 1$. The basic shapes of the dispersions are the same. But the magnetic flux with $\phi \in [0, 1/2)$ makes the left gap for Landau-Zener tunneling smaller or even closed and makes the right gap slightly bigger. For large t'/t, the magnetic field changes the dispersion dramatically [Figs. 2(d)–2(f)]. There will be a new smaller gap in the dispersion around $k \simeq -\pi/4$, and this gap can be

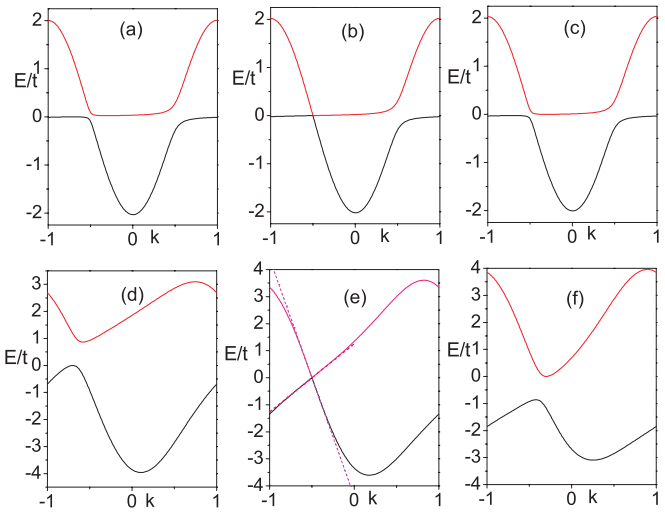

FIG. 2. (Color online) The single-particle dispersion for the no-driving-force system in the presence of magnetic field with (top) $t'/t = 0.15$ and (bottom) $t'/t = 1.5$ and (a) and (d) $\phi = 0.15$, (b) and (e) $\phi = 0.25$, and (c) and (f) $\phi = 0.35$. In (e) we also show the corresponding asymmetric Dirac cone. k is in units of $\pi/2$.

closed for particular ϕ. For different t'/t, $\phi = 1/4$ is a critical value, with the gap between two minibands being closed. After a straightforward calculation, one can get $E_+(k = -\pi/4, \phi = 1/4) = E_-(k = -\pi/4, \phi = 1/4) = 0$, and the gap closes at $k = -\pi/4$ for $\phi = 1/4$. Around the touch point the dispersion is almost linear [Fig. 2(e)], and there is an asymmetric Dirac cone in the dispersion for $\phi = 1/4$. After linearization, the form of the asymmetric Dirac equation reads

$$\epsilon_{\text{cone}}/t = v_{\pm}(k - k_0), \tag{7}$$

where $k_0 = -\pi/4$ is the Dirac point and $v_{+(-)}$ is the velocity of right (left) moving particles with

$$v_{\pm} = 2[-1 \pm \sqrt{1 + (t'/t)^2}]. \tag{8}$$

For comparison, we also plot the corresponding Dirac cone in Fig. 2(e), and around the touch point the two dispersions agree with each other very well.

Suppose that the system is filled by free fermions with half filling. When $\phi \neq 1/4$, the dispersion has a gap between two Bloch bands, and the system is a band insulator, while when $\phi = 1/4$, the gap closes and the system is a Luttinger liquid with gapless and linear low-energy excitations. Otherwise, there is magnetic flux in each triangle, and driven by it, particles should flow in the lattice. According to the continuity equation, the local current operators are given by [42]

$$\begin{aligned} \hat{J}^B_{2j-1} &= -it[c^\dagger_{2i-1}c_{2j+1} - c^\dagger_{2j+1}c_{2j-1}], \\ \hat{J}^Z_{2j} &= -it'[e^{-i\phi\pi}c^\dagger_{2j}c_{2j+1} - e^{i\phi\pi}c^\dagger_{2j+1}c_{2j}], \end{aligned} \tag{9}$$

where $\hat{J}^B_{2j-1}$ is the current operator along the baseline and $\hat{J}^Z_{2j}$ is the current operator along the zigzag path. In Fig. 3, we show currents of a system vs ϕ with $J_B = \langle \hat{J}^B_{2j-1} \rangle$ and $J_T = J_B + J_Z$. The structure of the picture is still the same for different t'/t. The currents are periodic in ϕ with the least common period being 1. Without magnetic flux the system has no current because there is no driving field. As ϕ increases, all

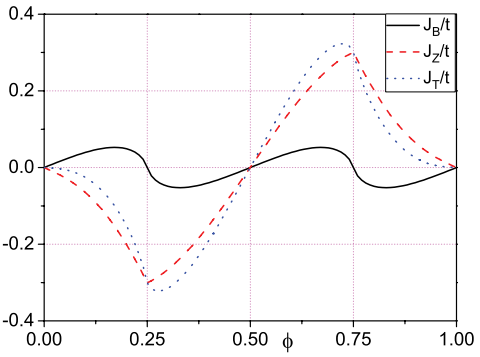

FIG. 3. (Color online) The currents J_B, J_Z, and J_T vs magnetic flux ϕ for the no-driving-force system filled by free fermions at half filling with $t'/t = 1$.

currents grow for small ϕ. In region $\phi \in (0, 1/4)$, the currents J_B and J_Z have opposite direction, and in each triangle there is a local current loop with nonzero total current J_T, while in region $\phi \in (1/4, 1/2)$, the currents J_B and J_Z have the same direction and all particles move along the same direction, with no local current loop. For $\phi = 1/4$, the system is a metal, but the current flows only along the zigzag path. It is worthwhile to notice that there is no zero J_T with finite J_B, so the magnetic field cannot drive the particles to form a local current in each triangle without drifting along the lattice. At $\phi = 1/2$ all the currents are zero, which should be related to the pure imaginary hopping amplitude along the zigzag path.

III. BLOCH-ZENER OSCILLATION AND RECONSTRUCTION

For a two-Bloch-band system under a driving force, it has been demonstrated that the dispersion of the system generally has the structure of two Wannier-Stark ladders [14]. On the other hand, after introducing the translation operator

$$T_m = \sum_j c^\dagger_{j-m} c_j \tag{10}$$

for two successive eigenstates (belonging to two different Wannier-Stark ladders) of the Hamiltonian H,

$$H|\varphi_0\rangle = E_0|\varphi_0\rangle, \quad H|\varphi_1\rangle = E_1|\varphi_1\rangle. \tag{11}$$

They satisfy the following relation:

$$H\{T_{2l}|\varphi_\alpha\rangle\} = \{E_\alpha + 2lF\}\{T_{2l}|\varphi_\alpha\rangle\} \tag{12}$$

with $\alpha = 0, 1$. Then, the eigenenergies of the Hamiltonian,

$$\begin{aligned} E_{0,n} &= 2nF, \\ E_{1,n} &= S + (2n+1)F, \end{aligned} \tag{13}$$

consist of two Wannier-Stark ladders with the corresponding eigenstates satisfying $\varphi_{\alpha,n} = T_2\varphi_{\alpha,n-1}$. The dynamics of a single-particle state under Hamiltonian H is a Bloch-Zener oscillation and is characterized by two periods (see the Appendix),

$$T_1 = \frac{\pi}{F}, \quad T_2 = \frac{2\pi}{F - |S|}. \tag{14}$$

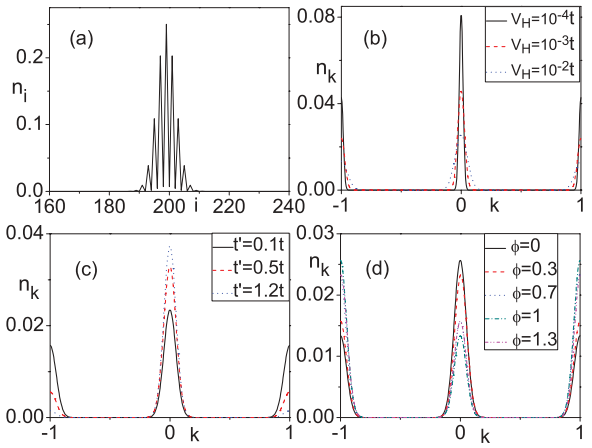

FIG. 4. (Color online) (a) The density profile for a particle in the trapped sawtooth lattice with $t'/t = 0.1647, V_H/t = 0.01$, and $\phi = 0$. (b) The momentum distribution of a particle in the trapped sawtooth lattice for different strengths of harmonic trap V_H with $t'/t = 0.1647$ and $\phi = 0$. (c) The momentum distribution of a particle in the trapped sawtooth lattice for different ratios t'/t with $V_H/t = 0.01$ and $\phi = 0$. (d) The momentum distribution of a particle in the trapped sawtooth lattice for different magnetic fluxes ϕ with $t'/t = 0.1647$ and $V_H/t = 0.01$. k is in units of π.

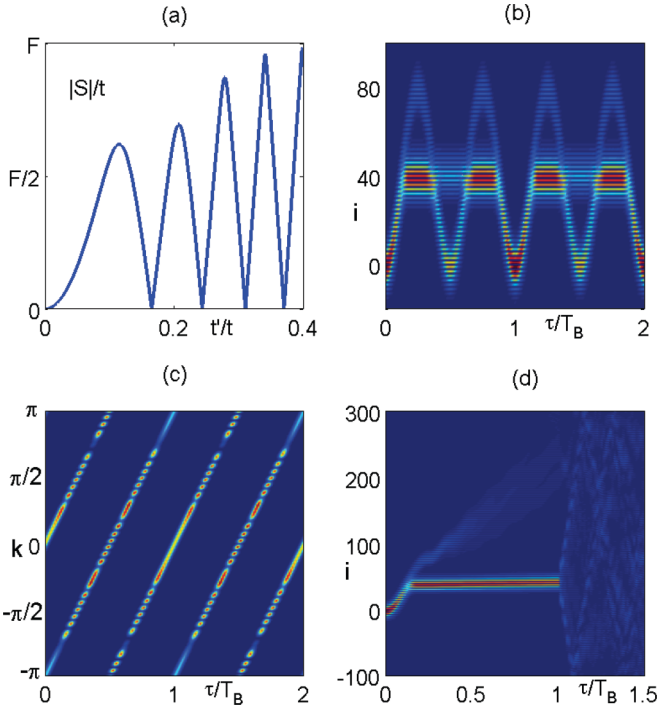

FIG. 5. (Color online) (a) $|S|$ vs t' for the driven sawtooth lattice with $F = 0.05t$. The dynamics of (b) the density profile and (c) the momentum distribution for a particle in the driven sawtooth lattice with $t'/t = 0.1647$, $F = 0.05t$, $V_H/t = 0.01$, and $\phi = 0$. (d) The dynamics of the density profile for producing the dynamical localized system with $t'/t = 0.1647$, $F = 0.05t$, $V_H/t = 0.01$, and $\phi = 0$.

In general, if T_1 and T_2 are commensurate, the single-particle state reconstructs at integer multiples of Bloch-Zener time (the least common period of T_1 and T_2).

In order to study the dynamics of a quantum particle in a driven sawtooth lattice, we need to prepare an initial state. At the beginning, by adding a harmonic trap into the system with the form

$$V_j = V_H(j - j_0)^2 \tag{15}$$

and letting the particle be in the single-particle ground state of the trapped system, a Gaussian-shaped single-particle wave packet around site j_0 can be formed. Here V_H is the strength of the harmonic trap, and j_0 is the position of the trap center. After turning off the harmonic trap and switching on the driving force, the wave packet will move.

For the initial trapped single-particle system, the density profile is Gaussian shaped, and there are many oscillations in it because of lattice frustration [Fig. 4(a)]. In Fig. 4 we also show the momentum distributions for systems with different strengths of the harmonic trap, ratio t'/t, and magnetic flux. For the system with zero magnetic flux, there is another peak around $k = \pm\pi$ in the momentum distribution [Fig. 4(b)], while there is only a Gaussian-shaped peak around $k = 0$ for the usual one-dimensional system. As V_H/t increases, the amplitude of both peaks at $k = 0$ and $k = \pm\pi$ decreases, and the extension of both peaks becomes larger. Eventually, the momentum distribution becomes flat, with the particle being localized at a single site for large enough V_H. On the other hand, as t'/t increases [Fig. 4(c)], the system trends to the usual one-dimensional system, and the peak at $k = \pm\pi$ becomes smaller while the peak at $k = 0$ becomes larger. The momentum distribution is periodic in ϕ with period 2. The presence of magnetic flux destroys the time-reversal symmetry of the system, and momentum distribution is usually asymmetrical, which is not obvious in the picture because of the small ratio t'/t [Fig. 4(d)]. Otherwise, for $\phi \in (0,1)$ the peak around $k = 0$ becomes smaller while the peak around $k = \pm\pi$ becomes larger as ϕ increases. For $\phi \in (1,2)$, the magnetic flux has the opposite effect.

Given an initial state, now we study the dynamics of a quantum particle in a driven sawtooth lattice without magnetic flux. Here we focus on the parameter region $t' \ll t$, whereas the single-particle dynamics for $t' > t$ is similar to that in the usual one-dimensional two-band systems with both Landau-Zener tunneling and Bragg scattering happening at the edge of the Brillouin zone (see Ref. [14]). In order to observe the reconstruction of the system, two periods T_1 and T_2 must be commensurate, which is decided by F and t'. In Fig. 5(a), we show numerical results of $|S|$ versus t' for a particular F. For different F, the structure of the picture is similar. In order to generate a particular Bloch-Zener time, t' must be one of the discrete numbers. For example, if we want $T_{BZ} = T_B$ for the system with $F = 0.05t$, we have to let $|S| = 0$ and then $t' = 0.1647t, \ldots$. T_{BZ} is the Bloch-Zener time, and T_B is the Bloch time for the usual one-dimensional system with $T_B = 2T_1$ [14]. On the other hand, numerical results show that the Landau-Zener tunneling probability [43] $P_{LZ} \approx \exp(-\frac{\pi\Delta^2}{8tF})$, where Δ is the gap for Landau-Zener tunneling defined above and $\Delta = 2t'\sqrt{2-(t'/t)^2}$ for $0 < t'/t < 1$. Then in order to see a clear sign of the Landau-Zener tunneling, we must choose small t' for a given driving force.

In Fig. 5, we also show the dynamics of the density profile and momentum distribution for a system without magnetic

flux. We choose $|S| = 0$ and let the system reconstruct at integer multiples of Bloch time T_B. From now on, we take Bloch time as the reference time scale. First of all, the density profile reconstructs at integer multiples of Bloch time [Fig. 5(b)]. After being released from the harmonic trap, the particle moves along the direction of the driving force. Around time $T_B/8$ it reaches the point $k \simeq \pi/4$, and Landau-Zener tunneling happens. Then part of the particle moves into upper excited Bloch band, while the other part of the particle remains in the lowest Bloch band and moves into the flat part. Because of Landau-Zener tunneling, the particle is divided into two parts, and they are separated in real space, with particles in the curve trajectory of the upper half of the picture being in the upper excited Bloch band. After Landau-Zener tunneling, particles which remain in the lowest Bloch band are localized in real space because of the partially flat band. At time $T_B/4$, the particle reaches the right edge of the Brillouin zone, changes the sign of momentum because of Bragg scattering, and moves against the direction of the driving force. Around time $3T_B/8$, the particle reaches the point $k \simeq -\pi/4$. Landau-Zener tunneling happens again, and particles in the flat part of the upper excited Bloch band are localized in real space. The particle changes its direction again at time $T_B/2$ and $k = 0$. As time goes on, more Landau-Zener tunneling and Bragg scattering happen. At time T_B the density profile resumes its original state.

In Fig. 5(c), we show the dynamical evolution of the momentum distribution for the same system as in Fig. 5(b). Particles with momenta in the interval $(-\pi/2,\pi/2)$ are in the lowest Bloch band, and outside the region particles are in the upper excited Bloch band. At time $\tau = 0$, there are two peaks in the momentum distribution with the peak at $k = \pm\pi$ being much smaller than at $k = 0$. The momentum of the particle is linear with time, with slope being given by the driving force F. After being released from the harmonic trap, the particle speeds up under the driving force, and it reaches the point $k \simeq \pi/4$ around time $T_B/8$. Landau-Zener tunneling happens between $k \simeq \pi/4$ in the lowest Bloch band and $k \simeq -3\pi/4$ in the upper excited Bloch band, and because of this the number of particles at $k \simeq \pi/4$ deceases and at $k \simeq -3\pi/4$ increases, which can be directly seen in the picture. From above we know that after Landau-Zener tunneling the particle in the lowest Bloch band is localized in real space because of the partially flat band, but the momentum of this particle is changing and finite. At time $T_B/4$ the particle reaches the right edge of the Brillouin zone, and because the number of particles in the lowest Bloch band at $k = \pi/2$ and the upper excited Bloch band at $k = -\pi/2$ are almost the same, after Bragg scattering, the momentum distribution has no obvious change. Around time $3T_B/8$ the particle reaches the point $k \simeq -\pi/4$. This Landau-Zener tunneling happens between $k \simeq -\pi/4$ in the lowest Bloch band and $k \simeq 3\pi/4$ in the upper excited Bloch band. At time T_B the momentum distribution resumes its original state.

From above we know that in the dynamics the particle in the flat band is localized in real space. Then a dynamical localized system can be created by keeping the system in the flat Bloch band all the time while changing the direction of the driving force at every time interval. For the system shown in Fig. 5(d), after the particle is released from the trap, the system evolves under the driving force, and around time $T_B/8$ part of the particle moves into the partial flat part of the lowest Bloch band, while the other part of the particle moves into the upper excited Bloch band and moves along the driving force. At time $T_B/4$ we change the direction of the driving force, and after this we change the direction for every time interval $T_B/16$ to let part of the particle always remain in the flat part of the lowest Bloch band. The other part of particle will move away from the localized one and will eventually leave the system. The remaining system is a dynamical localized one. In Fig. 5(d), we remove the driving force at time T_B, and the particle moves freely in the lattice. Right before the driving force is removed, the particle concentrates at the edges of Brillouin zone $k = \pm\pi/2$, and after the driving force is removed, the dynamical localized system is divided into two parts, and they move against each other linearly.

Now we study the effect of magnetic field on the dynamics. First of all, in the presence of magnetic flux, the system still has an energy spectrum with two Wannier-Stark ladders because of the two-Bloch-band dispersion for the corresponding no-driving-force system, and there is possible Bloch-Zener oscillation. But the magnetic flux changes the Bloch bands dramatically for the no-driving-force system, and it will change the value of $|S|$ and Bloch-Zener time. For two special points $\phi = 1/4,3/4$, the gap between two Bloch bands closes. After adding the driving force, there is only one Wannier-Stark ladder in the dispersion, and the system always reconstructs at

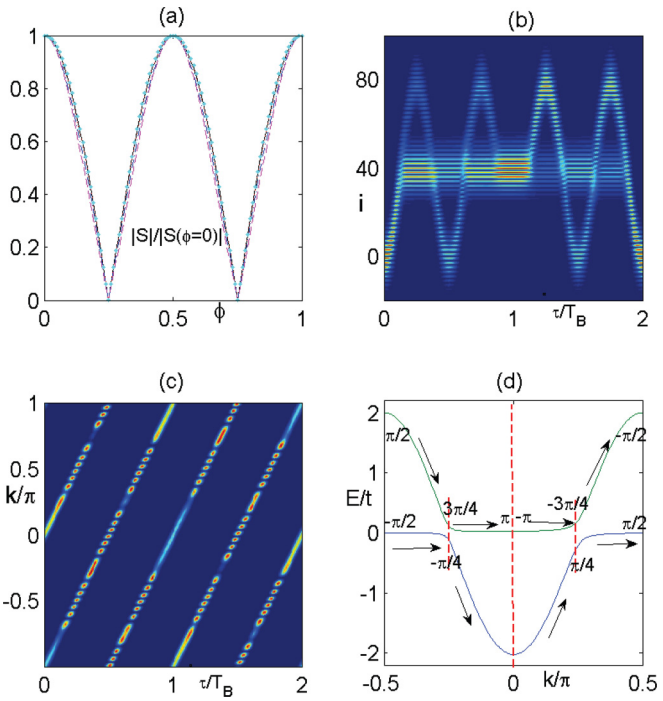

FIG. 6. (Color online) (a) $|S|/|S(\phi = 0)|$ vs ϕ for systems with small and different ratios t'/t [$|\cos(\phi 2\pi)|$, black straight line; $t'/t = 0.06$, red dotted line; $t'/t = 0.12$, blue dash-dotted line; $t'/t = 0.18$, magenta dashed line; $t'/t = 0.22$, cyan dots] and $F = 0.05t$. (b) The dynamics of density profile and (c) momentum distribution for a particle in the driven sawtooth lattice with $t'/t = 0.12, F = 0.05t$, $V_H/t = 0.01$, and $\phi = 0.096$. (d) The single-particle dispersion for the no-driving-force system in the presence of magnetic flux with $t'/t = 0.12$ and $\phi = 0.096$.

integer multiples of Bloch time (Bloch oscillation). For general ϕ, the system has a spectrum with two Wannier-Stark ladders, and there is Bloch-Zener oscillation. In order to study how the magnetic flux changes $|S|$, we plot $|S(\phi)/S(\phi=0)|$ vs ϕ for systems with small t'/t in Fig. 6(a). For large t'/t, the curve is different, and Landau-Zener tunneling probability is very small, which will cause no Bloch-Zener oscillation in the dynamics. In Fig. 6(a) we also show the curve $|\cos(\phi 2\pi)|$, and these curves agree with each other very well. So

$$|S(\phi)| = |\cos(\phi 2\pi) S(\phi=0)|. \tag{16}$$

Then, for example, for a system with $t' = 0.12t, F = 0.05t$, if we want Bloch-Zener time $T_{BZ} = 2T_B$, we can choose $\phi = 0.096$ in Eq. (16) to let $|S(\phi)| = F/2$ after getting $|S(\phi=0)|/t = 0.03045$. The dynamical evolution of the density profile and the momentum distribution are shown in Figs. 6(b), and (6 c), respectively. Obviously, the system really reconstructs at $\tau = 2T_B$. One can analyze in detail the Landau-Zener tunneling and the Bragg scattering with the help of Fig. 6(d).

IV. CONCLUSION

In summary, the dynamics of a quantum particle in the driven sawtooth lattice under uniform magnetic fields has been studied in this paper. First, we studied the spectral properties of a system in the absence of the driving force. Without magnetic field, the two-miniband system can be classified into three different types, with the shape of the Bloch bands being decided by the ratio t'/t, where t' (t) is the hopping amplitude along the zigzag path (baseline). Especially, with $t'/t \ll 1$, the system can host partially flat Bloch bands, which causes the dynamical localization in the dynamics of a particle in a driven system. In the presence of magnetic field, the gap between two minibands can be closed for some particular magnetic field, and when the gap is closed, the dispersion is an asymmetric Dirac cone around the touch point. We also studied the Bloch-Zener oscillation in the driven system with $t'/t \ll 1$. Landau-Zener tunneling and Bragg scattering happen at different times and places in the dynamics, and one can see the dynamical localization of a particle caused by the partially flat bands. Foremost, the system reconstructs at integer multiples of the Bloch-Zener time. The magnetic field changes the offset of two Wannier-Stark ladders in the spectrum of the driven system, then changes the Bloch-Zener time. But the Bloch-Zener oscillation still exists in the dynamics, and the system reconstructs at some time.

ACKNOWLEDGMENTS

This work has been supported by the NSF of China under Grants No. 11121063, No. 11174360, and No. 10974234, the National Program for Basic Research of MOST, and a 973 grant.

APPENDIX: DYNAMICS OF A PARTICLE IN A DRIVEN TWO-MINIBAND SYSTEM

For an initial state expanded in the Wannier-Stark basis,

$$|\Phi\rangle = \sum_n c_{0,n}|\Psi_{0,n}\rangle + \sum_n c_{1,n}|\Psi_{1,n}\rangle, \tag{A1}$$

the dynamics of $|\Phi\rangle$ under Hamiltonian H is given by

$$|\Phi(\tau)\rangle = \sum_n c_{0,n}e^{-iE_{0,n}\tau}|\Psi_{0,n}\rangle + \sum_n c_{1,n}e^{-iE_{1,n}\tau}|\Psi_{1,n}\rangle. \tag{A2}$$

Expanding Wannier-Stark functions in the Bloch basis,

$$|\Psi_{\beta,n}\rangle = \int_{-\frac{\pi}{2}}^{\frac{\pi}{2}} a_{\beta n}(k)|\chi_-(k)\rangle dk + \int_{-\frac{\pi}{2}}^{\frac{\pi}{2}} b_{\beta n}(k)|\chi_+(k)\rangle dk, \tag{A3}$$

and projecting $|\Phi(\tau)\rangle$ onto Bloch basis, one can get

$$\begin{aligned}\langle\chi_-(k)|\Phi(\tau)\rangle &= e^{-iE_0\tau}[a_{0,0}(k)C_0(k+F\tau) \\ &\quad + a_{1,0}(k)e^{-i(F+S)\tau}C_1(k+F\tau)], \\ \langle\chi_+(k)|\Phi(\tau)\rangle &= e^{-iE_0\tau}[b_{0,0}(k)C_0(k+F\tau) \\ &\quad + b_{1,0}(k)e^{-i(F+S)\tau}C_1(k+F\tau)],\end{aligned} \tag{A4}$$

where C_β are the Fourier series of $c_{\beta,n}$:

$$C_\beta(k+F\tau) = \sum_n c_{\beta,n}e^{-i2n(k+F\tau)}, \tag{A5}$$

which are π periodic. To get Eq. (A4) one has to use $T_{-2n}|\chi_\pm(k)\rangle = e^{-i2nk}|\chi_\pm(k)\rangle$ (translation of Bloch waves). From Eq. (A4), one can see that the dynamics of a particle is characterized by two periods: C_β are functions with a period of

$$T_1 = \frac{\pi}{F}, \tag{A6}$$

whereas the exponential function $e^{-i(F+S)\tau}$ has a period of

$$T_2 = \frac{2\pi}{F-|S|} \tag{A7}$$

because $e^{-i(F+S)\tau} = e^{-i2F\tau}e^{i(F-S)\tau}$. In general if T_1 and T_2 are commensurate,

$$\frac{T_1}{T_2} = \frac{F-|S|}{2F} = \frac{m}{n}, \quad n,m \in \mathbb{N}; \tag{A8}$$

thus the wave function reconstructs at integer multiples of Bloch-Zener time ($T_{\mathrm{BZ}} = nT_1$).

[1] F. Bloch, Z. Phys. **52**, 555 (1928).
[2] L. D. Landau, Phys. Z. Sowjetunion **2**, 46 (1932).
[3] C. Zener, Proc. R. Soc. London **137**, 696 (1932).
[4] M. Ben Dahan, E. Peik, J. Reichel, Y. Castin, and C. Salomon, Phys. Rev. Lett. **76**, 4508 (1996).
[5] M. Glück, A. R. Kolovsky, and H. J. Korsch, Phys. Rep. **366**, 103 (2002).
[6] E. Majorana, Nuovo Cimento **9**, 43 (1932).
[7] E. C. G. Stückelberg, Helv. Phys. Acta **5**, 369 (1932).

[8] J. Feldmann, K. Leo, J. Shah, D. A. B. Miller, J. E. Cunningham, T. Meier, G. von Plessen, A. Schulze, P. Thomas, and S. Schmitt-Rink, Phys. Rev. B **46**, 7252 (1992).
[9] T. Pertsch, P. Dannberg, W. Elflein, A. Bräuer, and F. Lederer, Phys. Rev. Lett. **83**, 4752 (1999).
[10] R. Morandotti, U. Peschel, J. S. Aitchison, H. S. Eisenberg, and Y. Silberberg, Phys. Rev. Lett. **83**, 4756 (1999).
[11] B. P. Anderson and M. A. Kasevich, Science **282**, 1686 (1998).
[12] B. Rosam, K. Leo, M. Glück, F. Keck, H. J. Korsch, F. Zimmer, and K. Köhler, Phys. Rev. B **68**, 125301 (2003).
[13] H. Trompeter, T. Pertsch, F. Lederer, D. Michaelis, U. Streppel, A. Bräuer, and U. Peschel, Phys. Rev. Lett. **96**, 023901 (2006).
[14] B. M. Breid, D. Witthaut, and H. J. Korsch, New J. Phys. **8**, 110 (2006).
[15] X.-G. Zhao, G. A. Georgakis, and Q. Niu, Phys. Rev. B **54**, R5235 (1996).
[16] M. C. Fischer, K. W. Madison, Q. Niu, and M. G. Raizen, Phys. Rev. A **58**, R2648 (1998).
[17] T. Hamada, J. Kane, S. Nakagawa, and Y. Natsume, J. Phys. Soc. Jpn. **57**, 12399 (1988).
[18] B. Doucot and I. Kanter, Phys. Rev. B **39**, 12399 (1989).
[19] T. Nakamura and K. Kubo, Phys. Rev. B **53**, 6393 (1996).
[20] D. Sen, B. S. Shastry, R. E. Walstedt, and R. Cava, Phys. Rev. B **53**, 6401 (1996).
[21] S. Chen, H. Buttner, and J. Voit, Phys. Rev. Lett. **87**, 087205 (2001); Phys. Rev. B **67**, 054412 (2003).
[22] S. Sarkar and D. Sen, Phys. Rev. B **65**, 172408 (2002).
[23] F. Monti and A. Sütö, Phys. Lett. A **156**, 197 (1991); Helv. Phys. Acta **65**, 560 (1992).
[24] M. E. Zhitomirsky and H. Tsunetsugu, Phys. Rev. B **70**, 100403 (2004).
[25] J. Richter, J. Schulenburg, A. Honecker, J. Schnack, and H. J. Schmidt, J. Phys. Condens. Matter **16**, S779 (2004).
[26] R. E. Walstedt, R. J. Cava, R. F. Bell, J. J. Krajewski, and W. F. Peck, Jr., Phys. Rev. B **49**, 12369 (1994).
[27] J. Schulenburg, A. Honecker, J. Schnack, J. Richter, and H. J. Schmidt, Phys. Rev. Lett. **88**, 167207 (2002).
[28] M. E. Zhitomirsky and A. Honecker, J. Stat. Mech. Theory Exp. (2004) P07012.
[29] O. Derzhko and J. Richter, Phys. Rev. B **70**, 104415 (2004).
[30] J. Schnack, R. Schmidt, and J. Richter, Phys. Rev. B **76**, 054413 (2007).
[31] C. Wu, D. Bergman, L. Balents, and S. Das Sarma, Phys. Rev. Lett. **99**, 070401 (2007).
[32] D. Jaksch and P. Zoller, Ann. Phys. (NY) **315**, 52 (2005).
[33] M. Lewenstern, A. Sanpera, V. Ahufinger, B. Damski, A. Sen(De), and U. Sen, Adv. Phys. **56**, 243 (2007).
[34] H. Tamura, K. Shiraishi, T. Kimura, and H. Takayanagi, Phys. Rev. B **65**, 085324 (2002).
[35] M. Ichimura, K. Kusakabe, S. Watanabe, and T. Onogi, Phys. Rev. B **58**, 9595 (1998).
[36] H. Ishii, T. Nakayama, and J. I. Inoue, Phys. Rev. B **69**, 085325 (2004).
[37] J. Richter, O. Derzhko, and A. Honecker, Int. J. Mod. Phys. B. **22**, 4418 (2008).
[38] O. Derzhko, A. Honecker, and J. Richter, Phys. Rev. B **79**, 054403 (2009).
[39] O. Derzhko, J. Richter, A. Honecker, M. Maksymenko, and R. Moessner, Phys. Rev. B **81**, 014421 (2010).
[40] A. Honecker and J. Richter, Condens. Matter Phys. **8**, 813 (2005).
[41] B. M. Breid, D. Witthaut, and H. J. Korsch, New J. Phys. **9**, 62 (2007).
[42] T. Shirakawa and E. Jeckelmann, Phys. Rev. B **79**, 195121 (2009).
[43] D. Witthaut, F. Trimborn, V. Kegel, and H. J. Korsch, Phys. Rev. A **83**, 013609 (2011).